Probe Rheology: A Simple Method to Test Tube Motion

Chen-Yang Liu,[†,‡] Adel F. Halasa,[⊥] Roland Keunings,*[,§] and Christian Bailly*[,†]

Unité de Chimie et de Physique des Hauts Polymères, Université catholique de Louvain, B-1348 Louvain-La-Neuve, Belgium, Key Laboratory of Engineering Plastics, Joint Laboratory of Polymer Science and Materials, Institute of Chemistry, Chinese Academy of Sciences, Beijing 100080, China, CESAME, Université catholique de Louvain, B-1348 Louvain-La-Neuve, Belgium, and Chemical Division R&D, Goodyear Tire and Rubber Company, Akron, Ohio 44305

Received July 11, 2006; Revised Manuscript Received August 9, 2006

ABSTRACT: We investigate the relaxation dynamics in the melt of entangled binary mixtures comprising a small fraction of short polybutadiene, polyisoprene and polystyrene chains in a high molecular weight (MW) matrix. In this way, we create model environments of quasi-permanent entanglements for probe chains, where tube motions are suppressed at the time scale of the probe chains reptation, while contour length fluctuations remain unaffected. The relaxation of a probe in its matrix presents several important features, which are independent of polymer species. Because of the absence of tube motions, the probe chains terminal peak is narrower, with a $G''(\omega) \sim \omega^{-1/2}$ high-frequency slope, in agreement with the prediction of pure reptation theory. Moreover, the position of the G'' peak, ω_{max} (rad/s), shifts to lower frequencies, which means that the longest relaxation time of the probe chains is increased, as compared to a melt of pure probe chains. Unambiguous and quantitative comparisons between the terminal times of probe chains in a matrix or self-melt environments are obtained with the help of an iso-free-volume correction. In this way, we clarify for the first time contributions from tube motions to the terminal relaxation. The retardation factor for the terminal relaxation time is independent of the number of entanglements Z above 100 but increases steadily below that threshold as $Z^{-0.3}$. The Z dependence of the retardation factor leads to different scalings for the terminal relaxation time of probe chains in self-melt or matrix environments. The observed scaling exponent of 3.1 in the matrix is very close to the prediction of the original reptation model. Our results hence indicate that the motions of surrounding chains have a dominant influence on the 3.4 exponent for terminal relaxation times and zero shear viscosity. This is in sharp contrast with the conventional view attributing the nonreptation scalings entirely to fluctuations but is in agreement with existing literature on tracer (probe) chains and self-diffusion.

1. Introduction

The most successful molecular theory describing the melt relaxation of entangled polymers is based on the reptation ideas proposed by de Gennes[1] and developed by Doi and Edwards.[2] The original reptation model considers one long linear chain trapped in a network of permanent entanglements. The network "obstacles" hinder lateral motions of the test chain for length scales larger than the network "mesh size", and confine the molecule within a 1D curvilinear tube. In real polymer melts, the situation is more complicated since two additional mechanisms must be considered for quantitative agreement. First, we need to account for the mobility of surrounding chains. Indeed, entanglements, i.e., topological obstacles formed by reptating chains, are not completely permanent. This is usually referred to as constraint release (CR) or "tube motions". In addition, contour length fluctuations (CLF), originating from springlike motions of the chain in its tube, are also important.

The effect of tube motions (due to the nonpermanent character of entanglements) on the relaxation of linear polymers is extremely subtle. The release of topological constraints will enable lateral motions of internal sections of the test chain,[3−5] which can be modeled as Rouse motions of the tube. Tube motion can lead to an enlarged "effective" tube diameter for the test chain on a coarse-grained time scale, leading to dynamic tube dilation ideas (DTD).[6−8] Tube dilation mechanisms are especially important for polydisperse and/or complex architecture polymer melts.[9,10] Several authors have addressed the validity limits of models based on tube Rouse motions and/or DTD.[9−13] However, all models should provide an accurate and self-consistent description for the simplest case, i.e., linear monodisperse melts. Different CR models,[5,12,14−16] the DTD model,[6] and the generalized double reptation model[17,18] all predict that tube motion accelerates the relaxation of linear polymers by a factor higher than 2 (2−3).

An important and unsettled question is whether the accelerating factor depends on molecular weight (MW) or not.[6,9,10] This issue is related to a long-standing problem with reptation theory. While pure reptation predicts a scaling exponent of 3.0 for the terminal relaxation time, τ_d, with respect to MW, the observed scaling is about 3.4 for real polymer melts.[19,20] Conventionally, tube models[16,21,22] credit the 0.4 difference primarily to CLF, with little or no influence from CR. However, any MW dependence of CR effects should affect the τ_d scaling. Recently, McLeish[10] has argued that MW-independence of CR effects might be idealistic considering that chain ends are responsible for correlated CR events in their vicinity.[23] Kavassalis and Noolandi[24−26] have described entanglements as a *collective* topological constraint, and taken into account the specific influence of chain ends on the entanglement network. Their model predicts a specific transition from the entangled to the unentangled state as chain length is shortened. In consequence, the relaxation time and plateau modulus will

* Corresponding authors. E-mail: christian.bailly@uclouvain.be (C.B); roland.keunings@inma.ucl.ac.be (R.K).
† Unité de Chimie et de Physique des Hauts Polymères, Université catholique de Louvain.
‡ Key Laboratory of Engineering Plastics, Joint Laboratory of Polymer Science and Materials, Institute of Chemistry, Chinese Academy of Sciences.
§ CESAME, Université catholique de Louvain.
⊥ Chemical Division R&D, Goodyear Tire and Rubber Company.

10.1021/ma061553i CCC: $33.50
Published on Web 09/19/2006

Table 1. Terminal Relaxation Data of Probes in "Permanent Network" Systems, Taken from the Literature

probes[a]	matrix[b]	type of network[c]	test method for τ_d[d]	retardation factor of τ_d	τ_d scaling in network	ref
PIB	BR	C	$\tau_{1/2}$	n.d.	3.0	29
EP	EPT	C	$\tau_{1/2}$	n.d.	3.5	30
PBD	(SB)n	B	$\omega_{maxG''}$	n.d.	3.1	31
PBD	SBS	B	$\tau_{1/2}$	~3	3.0	32
SB	PBD	C	$\tau_{1/2}$	10	3.4	33
PBD	PBD	C	$\tau_{1/2}$	>10	n.d.	34
PDMS	PDMS	C	$\tau_{1/2}$	10−100	n.d.	35
PI	NR	C	τ_{mg}	1	3.3	36
PI	NR	C	$\omega_{max\epsilon''}$	2.5	3.3	37
PBD	PBD	C	$\omega_{maxG''}$	1.9−3.2	3.35	38
PDMS	PDMS	C	$\omega_{maxtan\delta}$	n.d.	3.6	39
PBD	PBD	H	$\omega_{maxG''}$	2.0−3.0	3.3	40
PI	PI	H	$\omega_{max\epsilon''}$	2.0−4.0	3.0	49

[a] Key: PIB, polyisobutylene; EP, ethylene−propylene copolymer; PBD, polybutadiene; SB, styrene−butadiene copolymer; PDMS, poly(dimethylsiloxane); PI, polyisoprene. [b] Key: BR, butyl rubber; EPT, ethylene−propylene terpolymer; (SB)*n*, multichain styrene−butadiene block copolymer; SBS, styrene−butadiene−styrene block copolymer; NR, natural rubber. [c] Key: C, cross-linked; B, block copolymer; H, high MW. [d] Key: $\tau_{1/2}$, relaxation time for the portion of the modulus to decay to half of the plateau value; ω_{max}, frequency at which G'' or tan δ or ϵ'' has a maximum.

deviate from pure reptation scaling through the small MW dependence of the molecular weight between entanglements, M_e. This leads to MW-dependent CR dynamics. Similarly, different scalings vs MW are observed experimentally for entangled tracer ($D_{tr} \sim$ MW $^{-2.0}$) and self-chain diffusion coefficients ($D_s \sim$ MW $^{-2.3}$),[27,28] again suggesting a MW-dependent CR dynamics.

Experiments comparing the relaxation behavior of test chains in an environment of identical entangled chains or a permanent network are in principle an excellent way to answer two important and interrelated questions:

•How much longer is the terminal relaxation time τ_d in the absence of tube motions?

•What is the MW scaling for τ_d in a permanent network?

In the remainder of this paper, we use the term "self-melt" to describe a situation where test chains relax in an environment of identical chains, while we use the expression "probe chains" when the test chains are dispersed in a (quasi-)permanent network. Three techniques have been described in the literature to create a "permanent network" for probe chains:[1,20,29−40] (i) chemically cross-linked networks with a small fraction of linear chains,[29,30,33−39] (ii) microphase separated block copolymers with a high-T_g dispersed phase acting as cross-links and a low-T_g continuous phase with the same composition as the probe,[31,32] and (iii) a very high MW matrix with much longer reptation time than a probe of identical composition.[40] A compilation of published terminal relaxation data for probes in a "permanent network" is presented in Table 1. When tube motions are suppressed, retardation of the probe τ_d and narrow G'' peaks are observed, but the measured retardation factors are inconsistent, ranging from 3,[32,37−40] to 10,[33] or even higher,[34,35] depending upon the type of "network". The MW scaling exponent of the probe τ_d is also inconsistent, being either 3.0[29,31,32] or 3.4.[30,33,36−40] The reasons for the observed inconsistencies are explained below.

The most important problem concerning the published literature on "probe rheology" is the existence of (slight) differences in chemical composition between the "network" and/or the probe. These differences obscure the conclusions about relaxation times because the latter are very sensitive to variations of the monomeric friction coefficients, ζ_0. First, for diene-based chemical networks (polybutadiene (PBD), and polyisoprene (PI)), the cross-linking reaction takes place at high temperature. Even in the absence of oxygen, the formation of branched molecules and a broadening of the MW distribution of the probe are unavoidable because of side-reactions involving the double bonds. There are also differences from batch to batch for the cross-linking density.[39] In addition, static stress relaxation experiments have been used in most of the early studies[29,30,32−35] and are difficult to interpret because the contribution of the host network has to be subtracted from the probe relaxation. Second, for probes in block copolymers,[31,32] the inherent complexity of the systems also leads to inaccurate values of the probe τ_d. Finally, one paper only[40] describes the use of a high MW PBD matrix as "permanent network". However, an important parameter has been disregarded in the published study: the microstructure and hence the monomeric friction coefficients are not exactly the same for different probes. This effect has not been accounted for, resulting in uncertainty about the probe τ_d and corresponding retardation factor.

In this work, we investigate the relaxation dynamics of a small fraction (10%) of short probe chains in a high MW matrix and compare it with the behavior of the corresponding self-melts. Three polymers have been tested: 1,4-polybutadiene (PBD), 1,4-polyisoprene (PI) and polystyrene (PS). In all cases, particular care has been taken to carefully correct for the effect of minute variations of microstructure. This approach is referred to as "probe rheology". In this way, we create a model environment of "quasi permanent" entanglements for the probe chains, where tube motions are suppressed (at the time scale of the probe chains reptation) but reptation and CLF of the probe chains are otherwise unaffected. Comparing the relaxation dynamics of the probes in two environments, either as a self-melt or diluted in a high MW matrix, clearly reveal contributions of tube motions to the terminal relaxation.

2. Experiments

Narrow distribution linear 1,4-polybutadiene (1,4 addition > 90%), 1,4-polyisoprene (1,4 addition > 90%) and polystyrene were purchased from Polymer Source, Inc. Two additional PBD samples were obtained from Goodyear R&D Division. Molecular characterizations of the samples are provided in Table 2. Blends of 10% probe and 90% matrix mixed with 0.2% w/w Ciba IRGANOX B215 antioxidant were dissolved in excess solvent (toluene for PBD and PI, tetrahydrofuran for PS) over 2−3 days in the dark at room temperature with periodic manual stirring. Following complete dissolution of the polymers, solvent was driven off in a vacuum oven at room temperature for at least 1 week until the sample had less than 0.02% solvent left (as tested by weighing).

Linear viscoelastic (LVE) properties of the binary mixtures and the pure polymers were measured using a TA ARES rheometer with 8 mm diameter parallel-plate geometry. Because all blends containing 90% high MW matrix have very long relaxation times, special care was taken to ensure optimal loading of the samples. In particular, the PBD blends have been loaded and equilibrated at 25 °C. First, 10−15 layers of PBD cast films (with 50−100 μm thickness) are stacked on the lower fixture. Second, the upper fixture is lowered onto the sample until a normal force about 10 N is reached. Third, the edge of sample is carefully trimmed. Since the relaxation time τ_d of the PBD-1.2 M matrix is about 30 s at 25 °C as calculated from ω_{max}, a waiting period of more than 1 h (about 100 times τ_d) is used. After this period, the normal force exerted by the polymer on the fixtures has decayed below 0.2 N. Last, the edge of sample is carefully trimmed again.

Measurements were made under nitrogen atmosphere between 0.1 and 100 rad/s with 20 points per decade and temperatures ranging from +25 to −80 °C for PBD, from +25 to −40 °C for PI, and from 230 to 120 °C for PS. Repeated measurements at the

Table 2. Molecular Characterization and Terminal Relaxation Results

sample	ω_{max} of probe (rad/s) in melt	ω_{max} of probe (rad/s) in matrix	exptl retardation factor	T_g (°C)	iso-free volume correction	corrected retardation factor	M_w (kg/mol)	M_w/M_n	M_w/M_e [a]
PBD Matrix	0.035			−99.5			1240	1.13	792
PBD-14K	18 000	3500	5.14	−97.0	1.10	5.7	13.2	1.05	8.3
PBD-22K	5500	1300	4.23	−100	1.0	4.3	22.8	1.05	14.5
PBD-39K	550	185	2.97	−96.6	1.20	3.6	38.6	1.03	24.6
PBD-99K	24	9.5	2.50	−97.7	1.12	2.8	98.8	1.03	63
PBD-160K	4.5	2.0	2.25	−97.5	1.07	2.4	163	1.01	104
PBD-323K	0.47	0.4	1.17	−83.0	2.32	2.7	323	1.15	206
PBD-1.8K[b]							1.8	1.1	∼1
PI Matrix	0.0023			−62.5			1310	1.1	278
PI-82K	39	6.7	5.82	−66.5	0.80	4.7	81.8	1.07	17.3
PI-145K	8.7	2.0	4.35	−65.6	0.83	3.6	145	1.05	30.6
PS Matrix	0.038						1425	1.14	96.3
PS-234K	11.5	2.1	5.5				234	1.04	15.8

sample	exptl retardation factor	M_w of matrix (kg/mol)	M_w (kg/mol)	M_w/M_n	M_w/M_e [a]
PBD-41L[c]	4.2	174	40.7	1.04	25
PBD-41L[c]	4.5	435	40.7	1.04	25
PBD-98L[c]	3.2	435	97.5	1.04	62
PBD-100K[d]	2.8	410	99.1	1.01	63

[a] 1570 g/mol for PBD (ρ = 896 kg/m^3 at 25 °C), 4730 g/mol for PI (ρ = 900 kg/m^3 at 25 °C), 14 800 g/mol for PS (ρ = 959 kg/m^3 at 180°C.).[43,47] [b] Diluted matrix. [c] Obtained from ref 45. [d] Obtained from ref 46.

initial temperature after complete frequency sweep series did not show any significant change. The TA Orchestrator software was used to derive master curves at a reference temperature 25 °C for PBD and PI, 190 °C for PS, by a two-dimensional residual minimization technique.

3. Comparison of the Relaxation Dynamics of the Probe in Two Environments

The master curves for monodisperse PBD samples (self-melts) are presented in Figure 1a. The different PBD and PI samples used in this study do not have exactly the same microstructure, as can be inferred from the minor differences between the glass transition temperatures, T_g (see Table 2). Indeed, T_g of PBD and PI (and hence ζ_0 as well τ_e) correlate with the content of 1,2-addition units in the polymer (see also Figure 1 in ref 41). It is important to correct for these slight variations when comparing self-melts and matrix-probe chain systems. To this effect, we have used an "iso-free-volume state" correction according to Colby et al.[15] The reference system for this correction is the high MW matrix. The procedure is described in Appendix A. For matrix-probe chain systems, the low concentration of the probe chains (10%) makes this correction unnecessary.

Figure 1b shows the storage and loss moduli master curves for the 10% probe and 90% high MW matrix mixtures. The intermediate frequency G'' peaks correspond to the terminal relaxation of the probe in the mixtures. The consistency of the dynamic moduli is reflected by the excellent overlap of the high-frequency Rouse-like relaxation for all samples, and the identical WLF shift factors a_T and b_T as shown in Figure 1c. The corresponding WLF parameters are C_1 = 3.76, C_2 = 175 K. As a comparison, Figure 1c also shows the WLF shift factors found by Colby et al.[15] for high MW PBD samples (corresponding to C_1 = 3.48, C_2 = 163 K). The slight difference observed in the low-temperature range may come from a minor systematic deviation of the temperature control systems between the two rheometers. However, the second $G'-G''$ crossover point at high frequency, which is related to τ_e and ζ_0,[15,20] is very close to $\omega_C = 1.5 \times 10^7$ rad/s and $G_C = 2.5 \times 10^6$ Pa at 25 °C in both cases (see also Figure 3 in ref 15), which confirms the consistency between the two sets of data. It is worth noting that Colby's b_T data (and hence ours) are close to the standard ρT ratio shown in Figure13 of ref 15.

Typical master curves for the matrix, a representative probe self-melt (PBD-99K) and the corresponding probe−matrix mixture are shown in Figure 2. By comparison with the pure matrix in Figure 2a, the mixture presents two well-separated peaks for the loss modulus G'', corresponding to the terminal relaxations of the matrix and the probe. The frequency of the G'' maximum, ω_{max}, is connected to the longest relaxation time τ_d by the following simple relation.[38−40,42]

$$\tau_d = 1/\omega_{max} \quad (1)$$

In all cases except PBD-323K, the ratio between the matrix and probe relaxation times is above 100 because of the ratios of the component MWs are above 5 (roughly $5^3 > 100$). Therefore, the high MW matrix really acts as a permanent network at the time scale of the probe terminal relaxation. By comparison with the homopolymer self-melt in Figure 2b, the relaxation of the probe in the matrix presents two important differences. First, ω_{max} of the probe shifts toward lower frequencies, which means that τ_d of the probe is larger in the quasi-permanent network.[29−40] Second, the negative slope at the high-frequency side of the probe G'' peak is steeper in the matrix as compared to the self-melt, and hence the G'' peak is narrower.[38−40] Actually, the larger τ_d and narrower G'' peak are interrelated, and both result from the suppression of tube motions. This will be discussed in detail below.

To obtain the pure dynamic modulus of the probe in the matrix, the matrix contributions have to be subtracted. Here, we follow the procedure described by Ferry[32] and Roovers.[40] A matrix diluted with 10% very low-MW linear PBD ($M_w = 1.8 \times 10^3$ g/mol, $Z \sim 1$) was prepared and tested. The master curve of the diluted matrix is included in Figure 1b. The probe loss and storage moduli in a mixture were obtained by

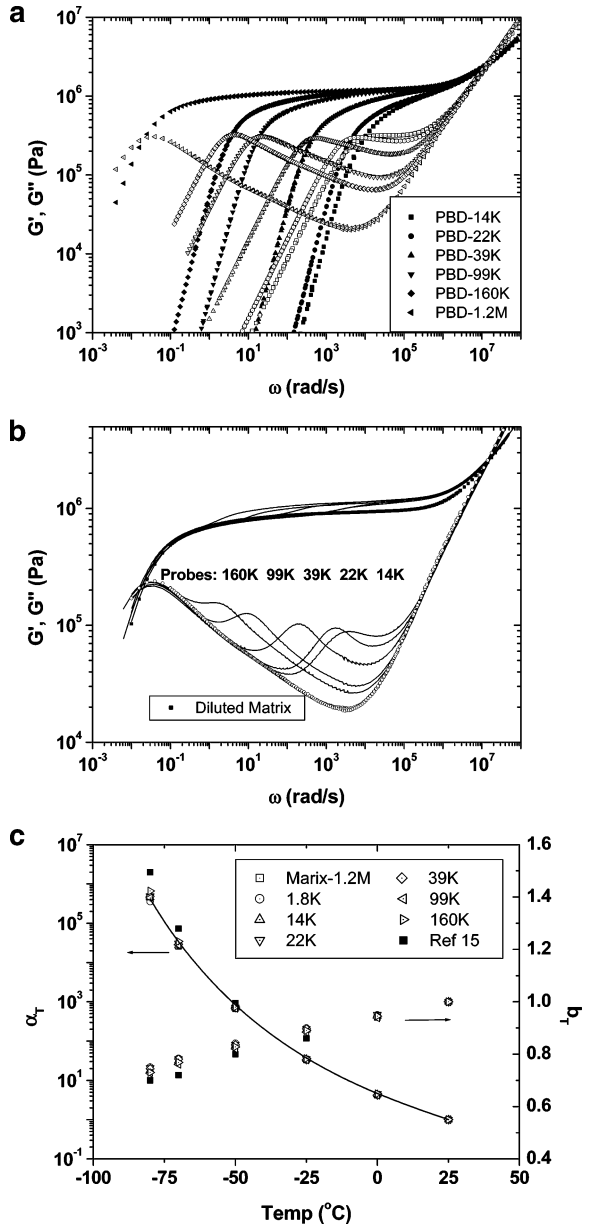

Figure 1. (a) Master curves of monodisperse PBD (160K, 99K, 39K, 22K, 14K) and high MW PBD-1.2M matrix. (b) Lines: master curves for the 10% PBD probe in high MW matrix systems. The small G″ peaks correspond to the relaxation of the probes in the matrix. Dots: matrix diluted with 10% very low-MW linear (PBD-1.8K) prepared for subtracting the matrix contribution. (c) WLF shift factors (open circles) of the matrix and probe-matrix mixtures as a function of temperature. The WLF parameters $C_1 = 3.76$, $C_2 = 175$ K at 25 °C, were obtained from the best fit (line) of all α_T data. Comparison with the WLF shift factors (filled squares) obtained from ref 15.

subtracting the corresponding moduli of the diluted matrix from the moduli of the mixture:

$$[G''(\omega)]_P = [G''(\omega)]_T - [G''(\omega)]_{DM} \quad (2)$$

where suffixes P, T, and DM refer to the probe, total mixture, and diluted matrix, respectively. This is almost equivalent to assuming that the probe acts as a short-chain solvent for the relaxation of the matrix thanks to the wide separation of the relaxation processes. The modulus subtraction procedure is in fact equivalent to a relaxation times spectrum subtraction when, as is the case here, the spectra of the long and short chains barely overlap each other. This assumption is essentially true

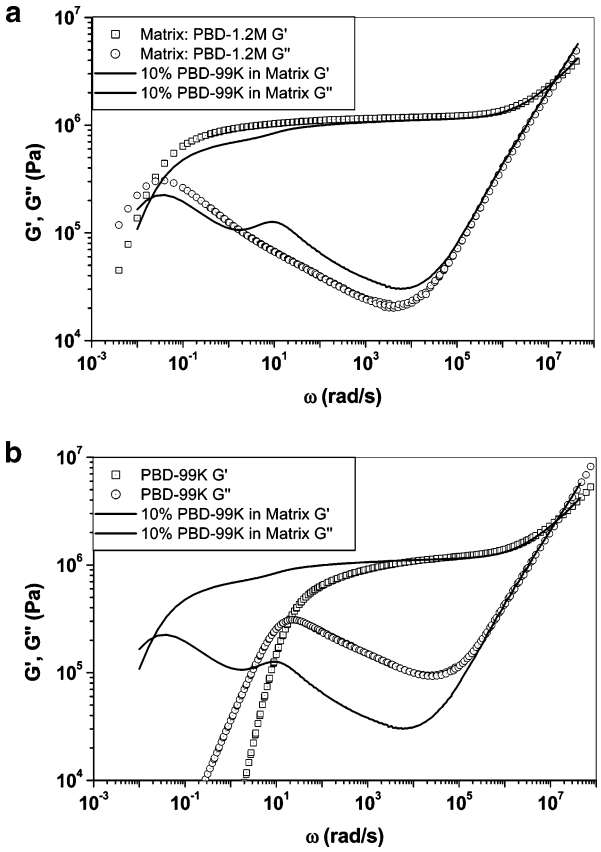

Figure 2. (a) Master curves for the PBD-1.2M matrix, and the representative PBD-99K probe-matrix mixture. (b) Master curves of the PBD-99K self-melt and the representative PBD-99K probe−matrix mixture.

for the shorter probes, but has some problems for the longer ones, especially PBD-323K.

The "probe dynamic moduli" of the PBD-99K, -39K, and -13K samples, calculated according to eq 2, are shown in Figure 3a. The G'' curve of the PBD-99K self-melt is also plotted as a reference. The corresponding curves for PBD-160K and -22K are shown in Figure 3b. Two important observations are can be made.

First, the terminal curves for all probes are *similar* to those of the corresponding self-melts (but not exactly the same): the well-known $G' \propto \omega^2$ and $G'' \propto \omega$ "terminal" regimes are indeed observed, and the first $G'-G''$ crossover frequency is close to the ω_{max} as it should be for monodisperse samples. The subtraction procedure is remarkable considering that the dynamic moduli curves of the five probes cover over 6 decades of frequency. Because the ratio of the component MWs is below 5 for the PBD-323K probe, the condition for valid use of eq 2 is not satisfied. Therefore, the probe modulus curves of PBD-323K are poor (not shown). The influence of the matrix is already noticeable for PBD-160K at low frequencies (Figure 3b). The probe plateau modulus $G_{N,probe}{}^0$ (high-frequency limit) ranges between 2.0×10^5 and 2.2×10^5 Pa. On the basis of simple dilution considerations:[9,10]

$$G_{N,probe}{}^0 = G_N{}^0(1 - \phi_{matrix}{}^2) \quad (3)$$

with $G_N{}^0$ the pure melt plateau modulus and ϕ_{matrix} the matrix volume fraction (=0.1). The dilution exponent is taken as 2. On the basis of eq 3, the measured probe plateau modulus is consistent with accepted values of $G_N{}^0$ for PBD: 1.05−1.15 MPa calculated compared to 1.15 MPa as reference value.[43]

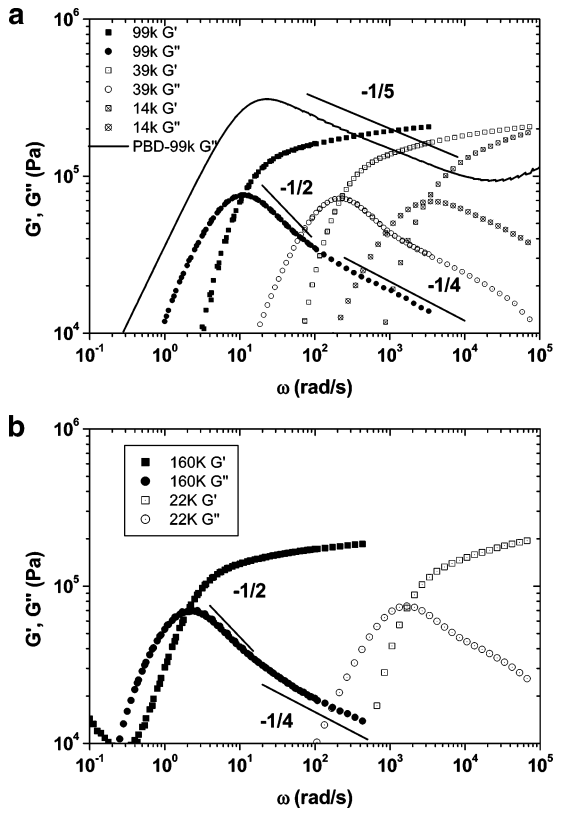

Figure 3. (a) Probe moduli for PBD-99K, -39K, and -14K: the G' and G'' moduli were obtained by subtracting the corresponding modulus of the diluted matrix from the total modulus of the mixture according to eq 2, as discussed in the text. The G'' curve of the PBD-99K self-melt is plotted as a reference. The $-1/2$ slope for G'' is the prediction of pure reptation theory,[1,2] and the $-1/4$ slope is the prediction with contour-length fluctuations.[16,21,22] The experimental slope for the PBD-99K self-melt is $-1/5$. (b) Probe moduli according to eq 2 for PBD-160K, and PBD-22K. The perturbing influence of the matrix is observed on the G'' curve of PBD-160K at the low frequencies.

A second important observation is that the shape of the probe loss peak for well-entangled samples, for instance PBD-99K and PBD-160K, is close to the prediction of pure reptation, i.e., a $\omega^{-1/2}$ power law for G'' at the right side of ω_{max}. This power law changes to $G'' \sim \omega^{-1/4}$ at higher frequencies, due to contour-length fluctuations.[16,21,22] To our knowledge, this is the first time that the reptation and CLF slopes are clearly observed for moderate MW samples. This of course results from the suppression of tube motions, which otherwise obscure the frequency separation of CLF and reptation relaxations. The probe G" peak is distinctly different from the corresponding self-melt, i.e., a $\omega^{-1/5}$ power law at the right side of ω_{max} for the PBD-99K self-melt (Figure 3a). An important point has to be kept in mind, namely that the effective mesh size of the diluted matrix is larger than the molecular weight between entanglements of monodisperse PBD at all relevant frequencies while this is only the case for the probe−matrix systems at frequencies lower than $1/\tau_{dprobe}$. This might affect the shape of the probe terminal peak at high frequencies in the CLF-dominated region. However, because of the low concentration of probe chains used (10%), this problem is not serious. The shape of G''_P will only be affected at the very high frequencies.[44] In particular, the location of the probe terminal peak maximum can be accurately determined and even the shape at higher frequency is preserved as discussed in section 5.

In summary, all results indicate that tube motions are indeed suppressed for all but the highest MW probe and that the matrix acts as a permanent network. We will compare the results of probe rheology with theoretical predictions of tube models in section 5. We now consider the retardation factor for τ_d.

4. Retardation Factors for τ_d in Self-Melt and High MW Matrix Environments

We call R the retardation factor for τ_d in the high MW matrix vs the self-melt environment:

$$R = \tau_{dProbe}/\tau_{dMelt} = \omega_{maxMelt}/\omega_{maxProbe} \quad (4)$$

with suffixes "Melt" and "Probe" referring to the self-melt and probe-matrix environments, respectively. An accurate determination of ω_{max} is required for the calculation of R. For the probe systems, we consider that all probe chains are diluted in the same matrix environment (i.e., have the same monomeric friction coefficient) and hence we apply no correction factor. Moreover, we obtain the same ω_{max} values if we either use the measured curves or the subtracted probe curve: the discrepancy between the two methods (with or without subtraction) is close to the experimental error of 0.05 log units (1.12 times), as shown in Figures 4a and 4b. For the self-melt environment, an iso-free-volume state correction[15] as described in Appendix A is required for the PBD and PI melts due to the small difference of microstructure between the probe chains and the matrix. On the other hand, the PS probe does not require any correction since there are no structural variations. For poorly entangled samples (PBD-14K and PS-234K), the accuracy of ω_{max} is further improved by removing the contribution of Rouse modes (taken as a power law extrapolation of the high-frequency data) from the experimental G'' curve.[43] This is shown in Figure 4, parts b and d. The obtained ω_{max} values in the matrix and self-melt environments, and the correction factors (when needed) are reported in Table 2. In all cases except PBD-323K, the correction factors are small (0.8−1.2) but crucial for the accuracy of the quantitative conclusion.

Figure 4 shows selected comparisons between the G'' terminal peaks of the probe and self-melt systems. For PBD-99K with $Z \sim 63$, the measured retardation factor R equals 2.5 (Figure 4a) and becomes 2.8 after adjustment for structural differences. On the other hand, for the short probe PBD-14K with $Z \sim 9$, the measured R equals 5.1 (Figure 4b) and becomes 5.7 after adjustment. The measured R is 5.8 for PI-82K with $Z \sim 17$ (Figure 4c) and the adjusted value is 4.7. The measured retardation factor is 5.5 for PS-234K with $Z \sim 16$ (Figure 4d) and requires of course no correction.

Rare results on binary mixtures from literature[45,46] have also been reanalyzed. Struglinski and Graessley[45] have investigated the linear viscoelasticity of a series of PBD binary mixtures with varying ratios of the high and low MW components. Figure 5 shows that ω_{max} of the short chains (the probe) decreases exponentially with increasing fraction of long chains (the matrix). Another set of results reported by Wang et al.[46] is also included in Figure 5 and follows the exact same trend. Two important observations can be made concerning Figure 5. First, because of the exponential dependence of $\omega_{maxProbe}$ with respect to blend composition, it is legitimate to obtain the retardation factor from a single measurement of a composition with a small fraction of probe chains. This validates our choice of 10% probe chains as a good compromise between (i) closeness to the "diluted probe" extrapolated value and (ii) experimental sensitivity limitations (no clear probe peak can be observed below 10%). Obviously, although 10% probe chains cannot be considered truly diluted in the matrix (in the sense that they still have some entanglements among themselves), this does not represent a critical limitation. Second, it is also worth noting

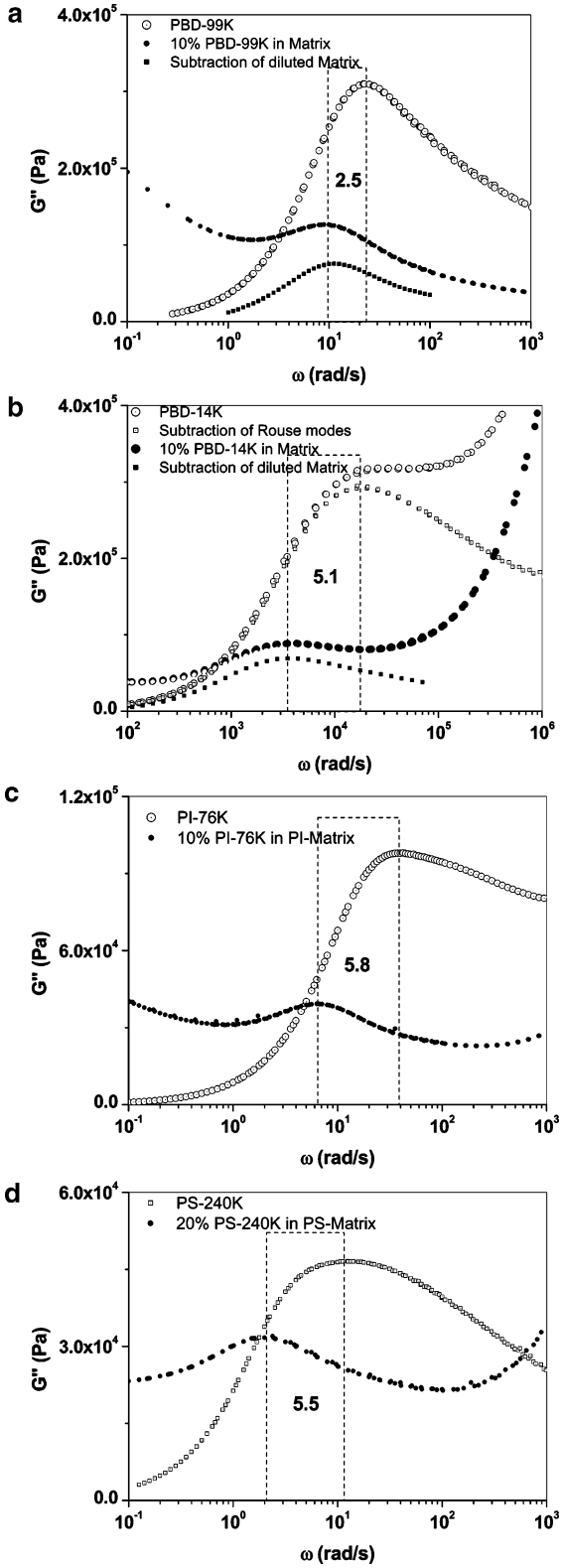

Figure 4. (a) Retardation of the probe in matrix relaxation peak for PBD-99K. Open circles: G'' self-melt. Filled circles: G'' probe in matrix. Filled squares: G'' probe modulus after subtracting the contribution of the matrix according to eq 2. (b) Retardation of probe in matrix relaxation peak for PBD-14K. Open circles: G'' self-melt. Filled circles: G'' probe in matrix. Filled squares: G'' probe modulus after subtracting the contribution of the matrix according to eq 2. Open squares: G'' of self-melt after subtraction of Rouse contribution.[43] (c) Retardation of the probe in matrix relaxation peak for PBD-76K. Open circles: G'' self-melt. Filled circles: G'' of probe in matrix. (d) Retardation of the probe in matrix relaxation peak for PS-240K. Open squares: G'' self-melt after subtraction of Rouse contribution.[43] Filled circles: G'' of probe in matrix.

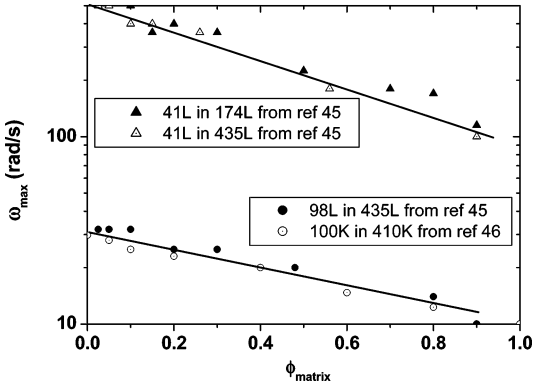

Figure 5. Angular frequency ω_{max} of peak maximum for probes as a function of matrix volumetric fraction. Data obtained from refs 45 and 46. See Table 2 for sample details.

that $\omega_{maxProbe}$ is independent of the matrix MW, once the blend components MW ratio is beyond 5. Indeed, for sample 41L, the retardations factors are indistinguishable in the two matrices (174L or 435L). Moreover, the observed retardation factors (4.2−4.5 for probe PBD with MW ∼ 40K and 2.8−3.2 for probe PBD with MW ∼ 100K) are in good agreement with our results for PBD-39K and PBD-99K.

All corrected R values listed in Table 2 are plotted as a function of entanglement number Z in Figure 6a. The MW between entanglements is taken as 1570 g/mol for PBD, 4730 g/mol for PI, and 14800 g/mol for PS.[43,47,48] All samples show a universal trend including two regions depending solely on Z: (i) for well-entangled chains with $Z > 100$, the retardation factor is independent of Z and has a value of about 2.5; (ii) at lower Z, the retardation factors are larger than 2.5 and increase as a power law with decreasing Z.

In a study on the dielectric relaxation of binary mixtures, Adachi et al.[49] have reported a similar MW dependence for the normal mode relaxation time of short polyisoprene probes in a high MW matrix. However, as already explained in the Introduction, no consistent trend for the retardation factor can be extracted from literature (Table 1) due to several types of experimental issues. An interesting example is the paper by Ndoni et al.[38] who have investigated the relaxation dynamics of PBD probes trapped in randomly cross-linked PBD networks. Retardation factors between 1.9 and 3.2 were found for probes with MW in the range 10−900 kg/mol and no obvious MW dependence of retardation factors was observed. Significant experimental problems have not been given proper consideration in ref 38. First, four linear PBD samples with *different* T_g (and hence ζ_0) were employed as network components, thus all networks are not strictly the same. In some cases, the T_g differences between the probe and the network are in excess of 10 °C (Figure 2 in ref 38), but no correction was reported. Second, different rheometers were employed for measuring the melts and networks, therefore systematic errors on temperature cannot be excluded. Last, the authors reported that the probe ω_{max} was not sensitive to the probe fraction in the range 10−50%, which is quite strange from a physics standpoint and contradicts the systematic trend observed in Figure 5.

Coming back to our work, the limiting retardation factor around 2.5 at high Z is in agreement with existing CR models,[5,12,14−16] as well as the DTD model[6] and the (generalized) double reptation model.[17,18]

At lower Z, the increasing retardation factors with decreasing Z point to an acceleration of tube motion and/or a gradual transition from the entangled to the unentangled state.[24−26] Actually, the retardation factor scales as $Z^{-0.3}$ for Z in the range

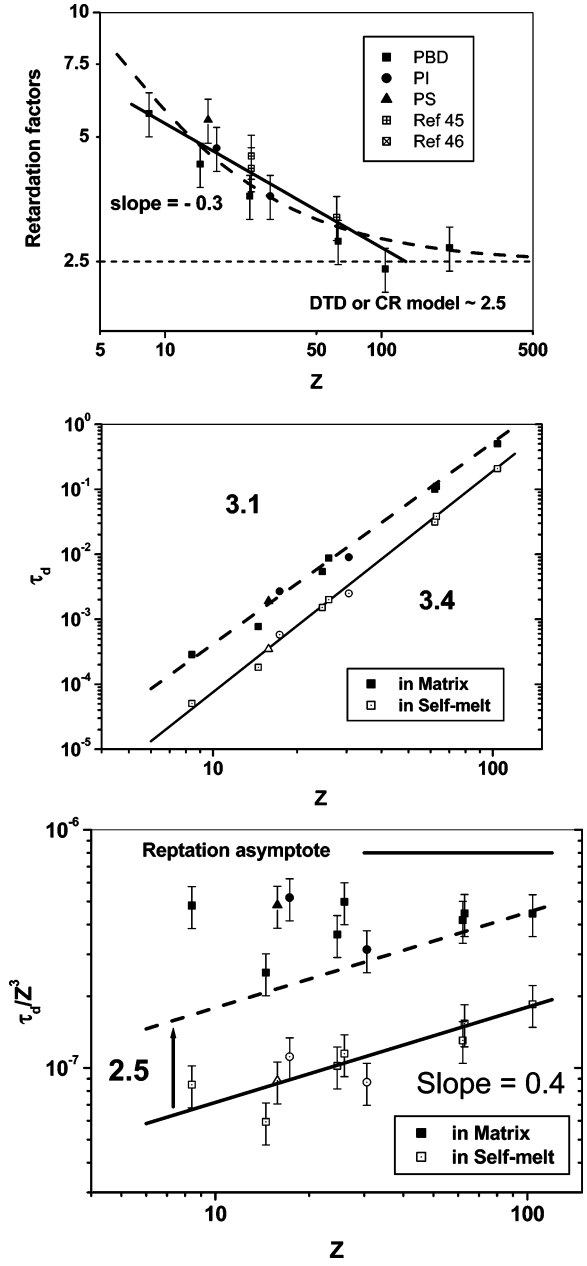

Figure 6. (a) Retardation factors of τ_d for probe chains in matrix as a function of the entanglement number Z. Retardation factors for additional PBD samples were extracted from refs 45 and 46. The horizontal dash-line represents the constant retardation factor about 2.5 predicted by the DTD model[6] for the well-entangled case. CR models[12,16] predict slightly different constant numerical values (around 3). The bold line represents the MW dependence of the retardation factor, as discussed in the text. The dotted line represents the fit by equation $R = 2.5(1 + 13/Z)$. (b) The longest relaxation time τ_d of the probe chains in two entangled environments (self-melt or matrix) as a function of entanglement number Z. The PI (circles) and PS (triangle) data were superimposed on the PBD (square) data by a vertical shift. (c) Data from Figure 6b replotted as τ_d/Z^3 vs Z to highlight deviations from the reptation scaling. The error bar is 20%, which is estimated conservatively as 10% for rheological test (τ_d) and 10% for MW (or Z). The horizontal line represents the reptation asymptote. The bold line represents a power law with a 0.4 slope for self-melts, the dash line corresponds to a constant retardation factor about 2.5.

10−100 (shown as the bold line in Figure 6a). Therefore, the Z dependence of the probe relaxation time in the high-MW matrix should be close to a power law with an exponent 3.1 = (3.4−0.3), because it is well-known that the viscosity of monodisperse PBD is proportional to $Z^{3.4}$.[15] The uncertainty on the slope is certainly less than 0.1, considering that even a −0.2 slope cannot

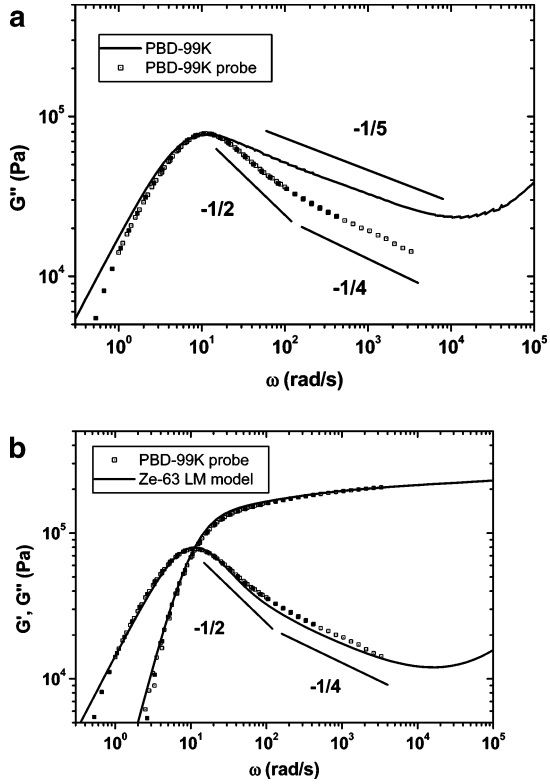

Figure 7. (a) Comparison between loss moduli of PBD-99K as probe and self-melt. The G'' peak for the self-melt was shifted to overlap both horizontally and vertically with the peak of the probe. (b) Comparison of G' and G'' curves for the PBD-99K probe and predictions of the LM model[16] with a constraint release parameter $c_v = 0$. The predicted curves with $Z = 63$ were shifted vertically and horizontally to overlap with the peak of the PBD-99K probe. The $-1/2$ slope for G'' is the prediction of original reptation theory,[1,2] and the $-1/4$ slope is the prediction of the contour-length fluctuations models.[16,21,22]

correctly represent the Z dependence of the retardation factor in Figure 6a. Our results clearly indicate a contribution of tube motions (i.e., the nonpermanence and/or imperfection of entanglements) on the τ_d scaling. So far, no CR model is able to predict this trend. Values of τ_{dMelt} and τ_{dProbe} are plotted as a function of Z in Figure 6b to highlight the change of scaling exponent. In Figure 6, PI and PS data are superimposed on the PBD data by an arbitrary vertical shift (obviously identical for all samples of the same polymer). As expected, the observed scaling exponent for the self-melt has the well-known 3.4 value. On the other hand, the scaling exponent for the probe is about 3.1, which is very close to the prediction of the original reptation model. The change of scaling is better revealed by plotting τ_d/Z^3 vs Z,[15,27] as shown in Figure 6c. In this format, the horizontal solid line represents the reptation asymptote, hence any deviations from the predicted Z^3 are clearly exposed. A slope of ∼0.1 is compatible with the probe results. It is important to keep in mind that any error on the MW of the samples will be emphasized in the τ_d/Z^3 vs Z plot. On the other hand, the R vs Z plot mostly screens out these errors since the retardation factor is a *relative* shift.

Since the permanent network only suppresses tube motions but does not affect CLF (in the classical view of tube models), our results prove that the contribution of CLF on the τ_d scaling is *quite weak*. If CLF effects were the dominating factor as expected by Doi,[21] the same scaling exponent of 3.4 would be observed even in the permanent network. A detailed comparison with CLF-dominated tube models will be carried out in the next Section. The weak CLF effect observed from τ_d scaling in the

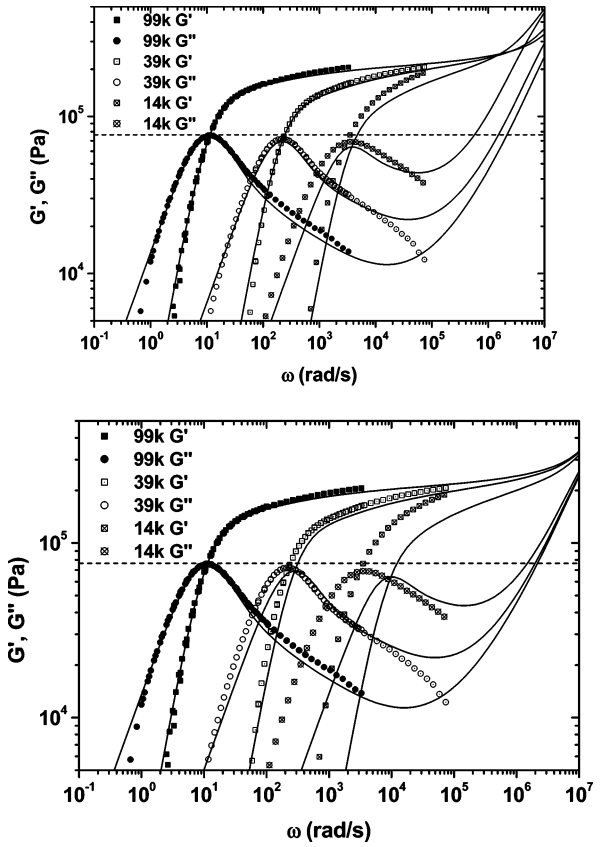

Figure 8. (a) Comparison between the G'' peaks of the probes and the predictions of the LM model for the PBD-99K, -39K, and -14K. The predicted G' and G'' curves with $Z = 63$ 24, 9 were shifted horizontally to overlap with the corresponding peaks of the probes by factors 5.2×10^6, 4×10^6, and 2×10^6. The vertical shift factor was fixed as $(1 - \phi_{matrix}^2)G_N^0$ (1.15 MPa for PBD). (b) Data from Figure 8a. The same horizontal shift factor, 5.2×10^6 (correct for PBD-99K), was used to move all predicted curves.

present work is consistent with the conclusion of our recent study about the Z dependence of the apparent plateau modulus,[50] and also consistent with the reptation scaling -2.0 observed in tracer diffusion.[27,28] The significant physics extracted from all experimental facts are discussed in detail in a separate paper.[51]

5. Comparison with Tube Models

Likhtman and McLeish[16] have recently developed a quantitative theory for the linear viscoelasticity of linear entangled polymers, which self-consistently combines CLF and CR with reptation (LM model). In this model, CR dynamics are controlled by a constraint release parameter c_v, with $c_v = 1$ corresponding to the Rubinstein−Colby model[12] and $c_v = 0$ to the complete absence of tube motions. Hence it is easy to switch off CR effects in the model by setting c_v to 0. Actual predictions of the LM model are available for Z ranging from 2 to 1000.[16] We therefore are able to compare our probe rheology results with the predictions of the LM model. We first compare the G'' peaks of the PBD-99K probe and self-melts in Figure 7a by freely shifting the melt curve so that it overlaps to the probe peak. As already discussed, the narrower G'' peak for the probe indicates the suppression of tube motions. We next freely shift the predicted curve of the LM theory for $Z = 63$ (based on $M_e = 1570$ g/mol) and $c_v = 0$ to overlap with the peak of the PBD-99K probe (Figure 7b). The agreement between the experimental results and predictions is striking for this highly entangled case. Theoretical predictions including CLF effects almost perfectly capture the relaxation dynamics of the probe chain in a high MW matrix, i.e., a reptation-controlled $\omega^{-1/2}$ power law at the immediate right side of ω_{max} and a CLF-controlled $\omega^{-1/4}$ power law at higher frequencies.[16,21,22]

We further compare the LM theory with our results for different PBD probes in Figure 8. We now fix the vertical shift factor as $(1 - \phi_{matrix}^2)$. G_N^0 according to the classical dilution relationship. G_N^0 is taken as 1.15 MPa.[43,47] For the horizontal scale, we freely shift the predicted G' and G'' curves ($Z = 63$, 24, 9) to overlap ω_{max} with the experimental results (Figure 8a). The corresponding shift factors are 5.2×10^6, 4×10^6, and 2×10^6 for PBD-99K, -39K, and -14K, respectively. Again, the agreement is excellent for the PBD-99K probe, which proves the empirical dilution relation is effective for the well-entangled case. However, predicted dynamic moduli are too low at high frequencies for the "short" probes. The most important discrepancy between the predictions and experiments is the second $G' - G''$ crossover, which correlates with the monomeric friction coefficient ζ_0 and the segmental time τ_e.[15,20] Alternatively, we can consider identical horizontal shift factors (corresponding to identical τ_e) for all samples. This is done in Figure 8b, where we use the correct value for PBD-99K (5.2×10^6). The predicted curves do not match the experiments well for the shorter probes, because the whole predicted G'' peaks follows a 3.4 exponent scaling, while the experimental peaks follow a 3.1 exponent scaling.

The mismatch is not difficult to understand, since the LM theory, as all current advanced tube models,[16,21,22] credits the 3.4 exponent scaling for η_0 and τ_d mainly to CLF, whereas CR or DTD only contribute a constant acceleration factor around 2.5−3.0.[6,12,16] To illustrate this, a retardation factor equal to 2.5 is plotted in Figure 6c (dashed line). The discrepancy with the experimental results is evident and has the same origin as the mismatch of the *whole* G'' peak for the shorter probes observed in Figure 8b, i.e., an overestimation of CLF effects.

6. Conclusion

By mixing a small fraction of short "probe" chains in a high MW matrix of the same composition, we have created model environments of quasi-permanent entanglements for the probe chains, where tube motions are suppressed at the time scale of the probe chains reptation, while contour length fluctuations remain unaffected. These model systems have been compared with pure probe chain melts ("self-melts"). As we use the same high MW matrix for all probe experiments and further apply an iso-free-volume state correction for the self-melts, we obtain unambiguous and quantitative comparisons for the first time. The relaxation of a probe in a high MW matrix presents several important features, which are independent of polymer species. Because of the absence of tube motions, the probe chains terminal peak is narrower, with a $G''(\omega) \sim \omega^{-1/2}$ high-frequency slope, in agreement with the prediction of pure reptation theory.[1,2] Moreover, the position of the G'' peak, ω_{max} (rad/s), shifts to lower frequencies, which means that the longest relaxation time τ_d of the probe chains is retarded, as compared to a melt of pure probe chains.

The retardation behavior of the τ_d exhibits two regions depending on Z. For well-entangled chains with $Z > 100$, the retardation factor is independent of Z and has a value about 2.5. This agrees with a generalized double reptation picture or DTD or Likhtman−McLeish models. At lower Z, the retardation factor is larger than 2.5 and increases with decreasing Z, approximately as $Z^{-0.3}$, which points to an acceleration of tube motions, presumably linked to a gradual transition from the entangled to the unentangled state.

The Z dependence of the retardation factor leads to different scalings for probe chains τ_d in self-melt or high MW matrix

environments. The scaling exponent of 3.1 for the probe in a high MW matrix is very close to the prediction of the original reptation model. Our results hence indicate that the motions of surrounding chains have a significant influence on the 3.4 exponent for τ_d and η_0. This is in sharp contrast with the conventional view attributing the nonreptation scalings entirely to fluctuations[16,21,22] but is in agreement with existing literature on tracer (probe) chains and self-diffusion.[27,28,51]

From the Z dependence of the apparent plateau modulus, we have recently found that current tube models overestimate the influence of CLF on the stress relaxation.[49] Now, we also find an over-reliance on CLF effects for the relaxation time (and confirm the stress scale problem). We conclude that the current tube models do not give enough credit to the effects of tube motions, in particular the MW dependence of CR effects for $Z < 100$. The observed Z dependence of the retardation factor R, of the order of $Z^{-0.3}$ for $10 < Z < 100$, is not accounted for in any existing model. Graessley[5] only predicts a rapidly vanishing Z^{-2} dependence because the characteristic constraint release time is proportional to $Z^2\tau_d$ for monodisperse polymers.

For poorly entangled chains, an important consideration is the very nature of entanglements. Kavassalis−Noolandi[24−26] have presented a *collective* picture of entanglements in terms of an average number of neighboring polymer segments restricting the lateral motion of the test chain. As chains get shorter, more and more dangling ends are present in the coordination sphere. Those ends are excluded from contributions to entanglements and their concentration scales as $\sim Z^{-1}$. A dilution effect by dangling ends is at least qualitatively in line with the experimental findings shown in Figure 6a. Indeed, we can fit the experimental results for the probe systems as

$$R = 2.5(1 + 13Z^{-1}) \tag{5}$$

This fit is shown in Figure 6a. Equation 5 would suggest that CR effects can be decomposed in a "limiting" MW-independent part (the 2.5 factor) and a MW-dependent effect indeed scaling as the concentration of chain ends. The prefactor is however very large, much larger than predicted from a straightforward chain ends dilution effect, which would rather lead to $R \propto (1 - Z^{-1})^{-1} \cong (1 + Z^{-1})$.

Finally, our probe rheology observations (summarized in Figure 6a) as well a wealth of studies on the relaxation of long chains in a low MW matrix,[52−54] reinforce the notion that CR is very complex. For the simple case of binary blends, the relaxation of the short chains is retarded by the long chains, and that of the long chains is accelerated by the short chains. Most efforts have focused on the latter effect,[9,10,52−54] while the former has received insufficient attention. A rigorous treatment of CR for polydisperse polymers undoubtedly remains a formidable task due to the intrinsic "many-body" nature of the problem.

Acknowledgment. This work has been supported by the ARC grant of the "Communauté française de Belgique". We are grateful to Dr. A. E. Likhtman for access to the theoretical predictions, and to Prof. W. W. Graessley for his valuable comments.

Appendix A. Iso-Free-Volume State Correction

For 1,4-polybutadiene and 1,4-polyisoprene (PBD and PI), slight differences in chemical microstructure, in particular 1,2-addition content,[41] are unavoidable between samples polymerized under different conditions. This results in different glass transition temperatures, T_g, hence different monomeric friction coefficients and segmental times at the same temperature.

Table 3. WLF Parameters for PBD Samples at $T_0 = 25$ °C, and the Respective T_g

	$C_1^{T_0}$	$C_2^{T_0}$	T_g	$C_1^{T_g}$ [a]	$C_2^{T_g}$ [b]
PBD-39K	3.91	172.8	−96	13.0	51.8
PBD-990K	3.78	172.8	−97.5	13.0	50.5
PBD-160K	3.83	174.1	−97.5	12.9	51.6
PBD-1.2M	3.76	175.3	−99	12.8	51.3

[a] $C_1^{T_g} = C_1^{T_0} \times C_2^{T_0}/C_2^{T_g}$. [b] $C_2^{T_g} = C_2^{T_0} + T_g - T_0$.

Therefore, the probe samples may have different segmental times in self-melt and high MW matrix environments, τ_{eMelt} and $\tau_{e\_in\_Matrix}$, if the probe and the matrix have different T_g (see Table 3). The T_g of the mixtures is very close to the T_g of the matrix because the matrix represents 90% of the mixture. Therefore, all probe-in-matrix terminal times can be compared without correction since the corresponding segmental times are identical. However, we are also interested in the self-melt terminal times in order to calculate the retardation factors. We need to correct those for differences in T_g. This can be done by the iso-free-volume state correction according to refs 15 and 55.

The terminal time τ_d can be considered as the product of the segmental time τ_e and a structural factor F:[15,20]

$$\tau_d = \tau_e F \tag{A-1}$$

The structural factor for monodisperse linear polymers depends on the number of entanglements only. The segmental time τ_e reflects the local dynamics, through the monomeric friction coefficient, and hence depends on the chemical structure and the temperature. Through the WLF equation, the self-melt segmental time τ_{eMelt} at a given temperature is related to τ_g, the segmental time at T_g:

$$\log\left(\frac{\tau_{eMelt}}{\tau_g}\right) = \frac{C_1^g[T - T_g]}{T - T_g + C_2^g} \tag{A-2}$$

Following refs 20 and 55, we assume that the WLF coefficients *referenced with respect to* T_g have the same values, C_1^g and C_2^g, for samples with very similar microstructure. The assumption can well be tested by the WLF parameters of PBD samples listed in Table 3. All experimental C_1^g and C_2^g data are close to the average values of 13.0 and 51.2.

Similarly, the probe segmental time in the matrix $\tau_{e\_in\_Matrix}$, follows:

$$\log\left(\frac{\tau_{e\ in\ Matrix}}{\tau_g}\right) = \frac{C_1^g[T - T_{g\ Matrix}]}{T - T_{g\ Matrix} + C_2^g} \tag{A-3}$$

Here T_{g_Matrix} is the T_g of the matrix. Finally, the correction factor $\tau_{eMelt}/\tau_{e\_in\_Matrix}$ at different temperatures, can be calculated by combining the two equations above since τ_g is the same.[20,55] The correction factors for τ_{eMelt} at 25 °C are listed in Table 2.

This procedure has been validated by two tests.

The shift factors calculated from eqs A-2 and A-3, and the correction factors $\tau_{eMelt}/\tau_{e\_in\_Matrix}$ have been plotted as a function of temperature for PBD-39K in Figure 9a. The correction factor decreases with increasing temperature. It takes the values 1.19 and 3.08 at +25 and −80 °C, respectively. The correction factor at −80°C could be checked independently from the comparison between the "self-melt" and "probe in matrix" high-frequency cross-points of G' and G'' (Figure 9b). Indeed, this frequency is correlated the segmental time.[15,20] We observe that the cross-point frequency for the PBD-39K self-melt is 3.2 times lower than that of the mixture, so the experimental correction factor

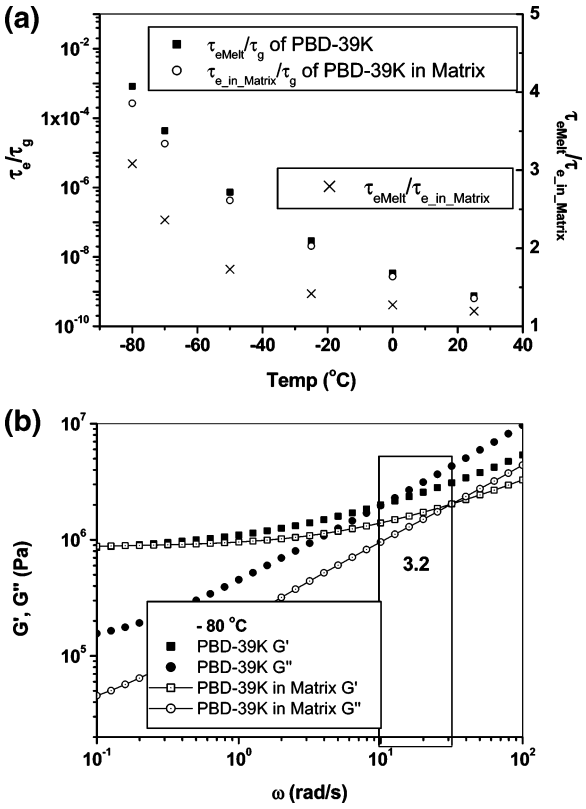

Figure 9. (a) Shift factors τ_e/τ_g and correction factors $\tau_{e\ Melt}/\tau_{e\_in\_Matrix}$ as a function of temperature for PBD-39K self-melt and probe in matrix. (b) Rheological data for PBD-39K self-melt and probe-matrix at −80 °C. The frequency of the G' and G'' cross-point is correlated with the segmental time τ_e.[15,20]

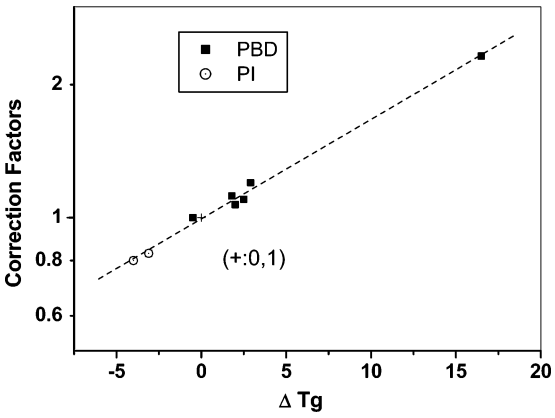

Figure 10. Correction factors at 25 °C for different PBD and PI samples plotted as a function of the T_g difference between the probe and the matrix.

$\tau_{eMelt}/\tau_{e\_in\_Matrix}$ should be 3.2, which is a good agreement with our calculated value of 3.08. The correction factors for other probes also could be checked by above method.

Second, the correction factors at 25 °C for different PBD and PI samples were plotted as a function of the T_g difference between the probe and the matrix (Figure 10). As expected, there is a good relationship between the correction factor and ΔT_g. In conclusion, the corrections for τ_{eMelt} are small in most cases (0.8−1.2) but crucial for the quantitative conclusion in this study.

References and Notes

(1) De Gennes, P. G. *J. Chem. Phys.* **1971**, *55*, 572. De Gennes, P. G. *Scaling Concepts in Polymer Physics*; Cornell University Press: Ithaca, NY, 1979.
(2) Doi, M.; Edwards, S. F. *The Theory of Polymer Dynamics*; Clarendon Press: Oxford, U.K., 1986.
(3) Klein, J. *Macromolecules* **1978**, *11*, 852.
(4) Daoud, M.; de Gennes, P. G. *J. Polym. Sci., Polym. Phys. Ed.* **1979**, *17*, 1971.
(5) Graessley, W. W. *Adv. Polym. Sci.* **1982**, *47*, 67.
(6) Marrucci, G. *J. Polym. Sci., Polym. Phys. Ed.* **1985**, *23*, 159.
(7) Ball, R. C.; McLeish, T. C. B. *Macromolecules* **1989**, *22*, 1911.
(8) McLeish, T. C. B. *J. Rheol.* **2003**, *47*, 177.
(9) Watanabe, H. *Prog. Polym. Sci.* **1999**, *24*, 1253.
(10) McLeish, T. C. B. *Adv. Phys.* **2002**, *51*, 1379−1527.
(11) Doi, M.; Graessley, W. W.; Helfand, E.; Pearson, D. S. *Macromolecules* **1987**, *20*, 1900.
(12) Rubinstein, M.; Colby, R. H. *J. Chem. Phys.* **1988**, *89*, 5291.
(13) Viovy, J. L.; Rubinstein, M.; Colby, R. H. *Macromolecules* **1991**, *24*, 4, 3587.
(14) Graessley, W. W.; Struglinski, M. J. *Macromolecules* **1986**, *19*, 1754.
(15) Colby, R. H.; Fetters, L. J.; Graessley, W. W. *Macromolecules* **1987**, *20*, 2226.
(16) Likhtman, A. E.; McLeish, T. C. B. *Macromolecules* **2002**, *35*, 6332.
(17) des Cloizeaux, J. *Macromolecules* **1990**, *23*, 4678; *J. Phys. (Paris), Lett.* **1984**, *45*, L17.
(18) Tsenoglou, C. *Macromolecules* **1991**, *24*, 1762.
(19) Graessley, W. W. *Adv. Polym. Sci.* **1974**, *16*, 1.
(20) Ferry, J. D. *Viscoelastic Properties of Polymers*, 3rd ed.; Wiley: New York, 1980.
(21) Doi, M. *J. Polym. Sci., Polym. Lett. Ed.* **1981**, *19*, 265. Doi, M. *Polym. Phys. Ed.* **1983**, *21*, 667.
(22) Milner, S. T.; McLeish, T. C. B. *Phys. Rev. Lett.* **1998**, *81*, 725.
(23) Klein, J. *Macromolecules* **1986**, *19*, 105.
(24) Kavassalis, T. A.; Noolandi, J. *Phys. Rev. Lett.* **1987**, *59*, 2674.
(25) Kavassalis, T. A.; Noolandi, J. *Macromolecules* **1988**, *21*, 2869.
(26) Kavassalis, T. A.; Noolandi, J. *Macromolecules* **1989**, *22*, 2709.
(27) Lodge, T. P. *Phys. Rev. Lett.* **1999**, *83*, 3218.
(28) Wang, S. Q. *J. Polym. Sci., Polym. Phys. Ed.* **2003**, *41*, 1589.
(29) Kramer, O.; Greco, R.; Neira, R. A.; Ferry, J. D. *J. Polym. Sci., Polym. Phys. Ed.* **1974**, *12*, 2361.
(30) Kramer, O.; Greco, R.; Ferry, J. D.; McDonel, E. T. *J. Polym. Sci., Polym. Phys. Ed.* **1975**, *13*, 1675.
(31) Kraus, G.; Rollmann, K. W. *J. Polym. Sci., Polym. Phys. Ed.* **1977**, *15*, 385.
(32) Kan, H.-C.; Ferry, J. D.; Fetters, L. J. *Macromolecules* **1980**, *13*, 1571.
(33) Nelb, G. W.; Pedersen, S.; Taylor, C. R.; Ferry, J. D. *J. Polym. Sci., Polym. Phys. Ed.* **1980**, *18*, 645.
(34) Taylor, C. R.; Kan, H.-C.; Nelb, G. W.; Ferry, J. D. *J. Rheol.* **1981**, *25*, 507.
(35) Granick, S.; Pedersen, S.; Nelb, G. W.; Ferry, J. D.; Macosko, C. W. *J. Polym. Sci., Polym. Phys. Ed.* **1981**, *19*, 1745.
(36) Poh, B. T.; Adachi, K.; Kotaka, T. *Macromolecules* **1987**, *20*, 2569.
(37) Poh, B. T.; Adachi, K.; Kotaka, T. *Macromolecules* **1987**, *20*, 2574.
(38) Ndoni, S.; Vorup, A.; Kramer, O. *Macromolecules* **1998**, *31*, 3353.
(39) Urayama, K.; Kawamura, T.; Kohjiya, S. *Macromolecules* **2001**, *34*, 8261.
(40) Roovers, J. *Polymer* **1989**, *30*, 2174.
(41) Carella, J. M.; Graessley, W. W.; Fetters, L. J. *Macromolecules* **1984**, *17*, 2775.
(42) Graessley, W. W. *J. Polym. Sci., Polym. Phys. Ed.* **1980**, *18*, 27.
(43) Liu, C. Y.; He, J. S.; Keunings, R.; Bailly, C. *Polymer* **2006**, *47*, 4461.
(44) Watanabe, H.; Matsumiya, Y.; Osaki, K.; Yao, M. L. *Macromolecules* **1998**, *31*, 7538.
(45) Struglinski, M. J.; Graessley, W. W. *Macromolecules* **1985**, *18*, 2630.
(46) Wang, S.; Wang, S. Q.; Halasa, A.; Hsu, W. L. *Macromolecules* **2003**, *36*, 5355.
(47) Fetters, L. J.; Lohse, D. J.; Richter, D.; Witten, T. A.; Zirkel, A. *Macromolecules* **1994**, *27*, 4639.
(48) Larson, R. G.; Sridhar, T.; Leal, L. G.; McKinley, G. H.; Likhtman, A. E.; McLeish, T. C. B. *J. Rheol.* **2003**, *47*, 809.
(49) Adachi, K.; Itoh, S.; Nishi, I.; Kotaka, T. *Macromolecules* **1990**, *23*, 2554.
(50) Liu, C. Y.; He, J. S.; Keunings, R.; Bailly, C. *Macromolecules* **2006**, *39*, 3093.
(51) Liu, C. Y.; Keunings, R.; Bailly, C. Do Deviations from Reptation Scaling of Entangled Polymer Melts Result From Single or Many Chain Effects? Submitted for publication.
(52) Leonardi, F.; Allal, A.; Marin, G. *J. Rheol.* **2002**, *46*, 209.
(53) Watanabe, H.; Ishida, S.; Matsumiya, Y.; Inoue, T. *Macromolecules* **2004**, *37*, 6619.
(54) Park, S. J.; Larson, R. G. *J. Rheol.* **2006**, *50*, 21.
(55) Pathak, J. A.; Kumar, S. K.; Colby, R. H. *Macromolecules* **2004**, *37*, 6994.

MA061553I